Environmental Science & Technology

pubs.acs.org/est

Article

Incorporating Cooking Emissions To Better Simulate the Impact of Zero-Emission Vehicle Adoption on Ozone Pollution in Los Angeles

Qindan Zhu,* Rebecca H. Schwantes,* Chelsea E. Stockwell, Colin Harkins, Congmeng Lyu, Matthew Coggon, Katelyn A. Yu, Carsten Warneke, Jordan Schnell, Jian He, Havala O. T. Pye, Meng Li, Ravan Ahmadov, Eva Y. Pfannerstill, Bryan Place, Paul Wooldridge, Benjamin C. Schulze, Caleb Arata, Anthony Bucholtz, John H. Seinfeld, Lu Xu, Kristen Zuraski, Michael A. Robinson, J. Andrew Neuman, Jessica Gilman, Aaron Lamplugh, Patrick R. Veres, Jeff Peischl, Andrew Rollins, Steven S. Brown, Allen H. Goldstein, Ronald C. Cohen, and Brian C. McDonald

Cite This: *Environ. Sci. Technol.* 2025, 59, 5672−5682

Read Online

ACCESS | Metrics & More | Article Recommendations | Supporting Information

ABSTRACT: Despite decades of emission control measures aimed at improving air quality, Los Angeles (LA) continues to experience severe ozone pollution during the summertime. We incorporate cooking volatile organic compound (VOC) emissions in a chemical transport model and evaluate it against observations in order to improve the model representation of the present-day ozone chemical regime in LA. Using this updated model, we investigate the impact of adopting zero-emission vehicles (ZEVs) on ozone pollution with increased confidence. We show that mitigating on-road gasoline emissions through ZEV adoption would benefit both air quality and climate by substantially reducing anthropogenic nitrogen oxides (NO_x) and carbon dioxide (CO_2) emissions in LA by 28 and 41% during the summertime, respectively. This would result in a moderate reduction of O_3 pollution, decreasing the average number of population-weighted O_3 exceedance days in August from 9 to 6 days, and would shift the majority of LA, except for the coastline, into a NO_x-limited regime. Our results also show that adopting ZEVs for on-road diesel and off-road vehicles would further reduce the number of O_3 exceedance days in August to an average of 1 day.

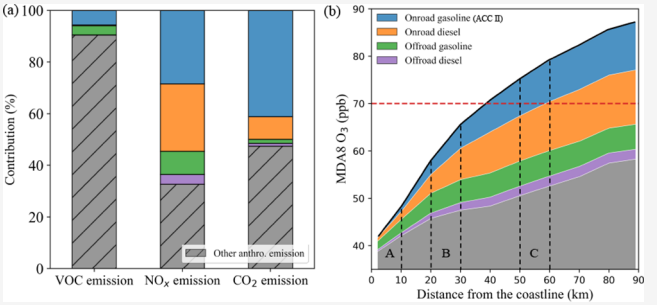

KEYWORDS: *cooking VOC emissions, urban O_3 pollution, zero emission vehicle adoption, CO_2 emissions*

1. INTRODUCTION

Automobiles emit criteria air pollutants and greenhouse gases. They emit nitrogen oxides (NO_x) and volatile organic compounds (VOCs), which undergo further reactions to form secondary pollutants including secondary organic aerosols and ozone (O_3).[1] These secondary pollutants have been associated with an increased risk of premature mortality.[2−7] Moreover, automobiles stand out as one of the largest contributors to anthropogenic greenhouse gas (GHG) emissions in the United States, accounting for 17% of total GHG-equivalent emissions in 2022.[8] The substantial radiative impact of long-lived GHGs emitted from anthropogenic sources has resulted in a 1.1 °C global surface temperature increase above preindustrial levels,[9] leading to large changes in weather and climate extremes,[9] including more frequent and extreme wildfires due to heat and drought, which also negatively impact air quality.[10,11]

California experiences the most severe O_3 pollution in the United States.[12] To address urban air pollution and the effects of climate change, California has set targets for Zero-Emission Vehicle (ZEV) adoption through electrification of vehicles.[13] California issued executive order N-79-20 in 2020, followed by the Advanced Clean Cars II (ACC II) regulation launched in 2022, to establish a year-by-year roadmap to phase out gasoline-powered cars by requiring sales of all new passenger vehicles to be zero-emission by 2035. California's policy has been adopted in other states and nations to accelerate ZEV adoption, including New York,[14] Massachusetts,[15] the United Kingdom,[16] and the European Union.[17]

Previous studies have quantified the impact of ZEV adoption on ambient air quality and the corresponding health outcomes and environmental equity.[18−25] While these studies agree on the benefit of ZEV adoption in reducing the levels of NO_x,

Received: January 19, 2025
Revised: February 11, 2025
Accepted: February 12, 2025
Published: March 12, 2025

CO, and $PM_{2.5}$, the changes in the level of O_3 pollution remain uncertain. The sensitivity of O_3 to ZEV adoption is quantified using chemical transport models configured with contrasting emission scenarios. While most studies find improvements in peak O_3 on the order of 1−5 ppb,[19,20,23,26] Li et al.[25] showed that 100% renewable electricity scenarios could lead to 5% increases in ozone concentration relative to a 2012 baseline year in Los Angeles (LA). The reported opposite trends in O_3 following ZEV adoption are attributed to the nonlinearity in O_3 formation and highlight the importance of accurately representing the mixture of VOCs and NO_x that govern ozone photochemistry.

Compared to urban NO_x emissions, which are well-documented and evaluated in Yu et al.,[27] VOC emissions are more complex due to the diverse mix of biogenic and anthropogenic sources. The anthropogenic VOC sources include vehicular emissions, volatile chemical products (VCPs), and cooking VOC emissions. Recent research has unveiled substantial underestimations in cooking VOC emissions within current emission inventories, suggesting that cooking VOC emissions may be a significant missing source for VOC_r. While the National Emission Inventory (NEI) suggests that cooking contributes to less than 1% of urban VOCs, Coggon et al.[28] show that cooking may account for as much as 20% of the total anthropogenic VOC emissions for Las Vegas.

In this study, we update a chemical transport model, the Weather Research and Forecasting with Chemistry version 4.2.2 (WRF-Chem), to incorporate cooking VOC emissions and chemistry. These updates alter the chemical regimes that impact ozone production and better represent ground, mobile, and aircraft observations of VOCs. We demonstrate that the updated model simulation yields an improved representation of O_3 chemistry, allowing for comprehensive sensitivity analysis of changes in O_3 due to ZEV adoption in the LA Basin. The results provide insight into how the current ACC II regulation can change the ambient O_3 abundance and alter the O_3 formation chemical regimes and can be used to inform further strategies designed to reduce O_3 pollution in the LA Basin.

2. MATERIALS AND METHODS

2.1. Observations. We utilize five sets of observations to validate cooking emissions and evaluate the model performance in representing O_3 chemistry, as discussed in detail in Section 4 of Zhu et al.[29] The first observation was the airborne measurement during the RECAP-CA (Re-evaluating the Chemistry of Air Pollutants in California) field campaign, which occurred between June 1−22, 2021, at 300−400 m above ground. The second and third observations were mobile laboratory and ground site measurements during the SUNVEx (Southwest Urban NO_x and VOC Experiment) field campaign in August and early September 2021. The last two observations were the hourly ozone measurements from 12 Air Quality System (AQS) monitoring sites reported by the U.S. Environmental Protection Agency (EPA) over Los Angeles, and the HCHO measurements from five South Coast Air Quality Management District (SCAQMD) monitoring sites. Among all observations, the RECAP-CA airborne and SUNVEx mobile measurements are segregated into four regions following Pfannerstill et al.[30] and Nussbaumer et al.,[31] including Downtown LA, San Bernadino Valley, Santa Ana Valley, and Coastal LA. The measurements of VOCs, CH_4, CO, and NO_y analyzed in this study and the corresponding instruments are summarized in Table S1. We account for only a subset of VOCs that are calibrated with an associated observational uncertainty of 30%, including CH_4, methanol, ethanol, acetaldehyde, acetone, isoprene, MACR, MVK, monoterpenes, benzene, toluene, benzaldehyde, xylene, nonanal, and octanal. MELODIES MONET (https://melodies-monet.readthedocs.io/) was used to pair the surface and aircraft observations with the model results.[32]

2.2. Emission Inventory. The baseline emissions for pollutants except for cooking emissions are described by Zhu et al.[29] The fossil fuel CO_2 emissions are from the GReenhouse gas And Air Pollutant Emission System (GRA^2PES) emission inventory and are described in https://csl.noaa.gov/groups/csl4/gra2pes/ and Lyu et al.[33] The GRA^2PES emissions inventory is a further development of the anthropogenic emissions inventory used most recently by Zhu et al.[29] This development adds complete anthropogenic fossil fuel CO_2 emissions generated from a common framework to air pollutant emissions. In general, GRA^2PES incorporates previously developed fuel-based inventories of mobile source emissions.[34] Residential and commercial building emissions are from the US Energy Information Administration's (EIA) State Energy Database System (SEDS) and downscaled with building CO emissions from the US NEI. Point source emissions are similarly calculated from SEDS and downscaled using CO emissions from the NEI. For facilities where data are available at a facility level, CO_2 emissions are taken from the US Greenhouse Gas Reporting Program (GHGRP) and Continuous Emissions Monitoring Systems (CEMS) of power plants. The GRA^2PES CO_2 emissions are presented here to quantify the maximum potential reduction of fossil CO_2 emissions from ZEV adoption and simulate GHG and air quality co-benefits.

2.2.1. Estimate of Cooking VOC Emissions. The estimation of cooking VOC emissions is based on observations. Coggon et al.[28] utilized VOC observations from SUNVEx mobile measurements in downtown Las Vegas, NV, and applied positive matrix factorization (PMF) analysis to allocate the VOCs to cooking sources. To derive the cooking VOC emission over LA, we calculate the cooking VOC emissions per capita to be 15.707 g of VOC/person/day based on observations in Las Vegas and scale it with the population map in LA.

Additionally, we identify two VOC species as tracers of cooking emission, octanal and nonanal. Attributing them exclusively to cooking emissions leads to the ratio of ethanol to nonanal of 6.7. It is worth noting that this ratio is significantly lower than those estimated from other observations.[35,36] Pfannerstill et al.[35] estimated the spatial distribution of VOC emissions using airborne flux measurements over LA and utilized footprint and multilinear regression to separate the contributors of sources.[30] Among the VOC fluxes with a cooking emissions profile, the ratio of ethanol to nonanal varies between 27 and 75 with a median value of 37. A similar ratio, 40.2, is reported in another independent indoor measurement from the HOMEChem experiments.[36,37] Therefore, we further increase the ethanol emission to match the ratio of ethanol to nonanal to 37, aiming for better agreement with RECAP-CA and HOMEChem observations (see Section S2.5 for more details). The modified cooking VOC emissions per capita that account for scaling up ethanol emissions are 25.155 g of VOC/person/day.

https://doi.org/10.1021/acs.est.5c00902
Environ. Sci. Technol. 2025, 59, 5672−5682

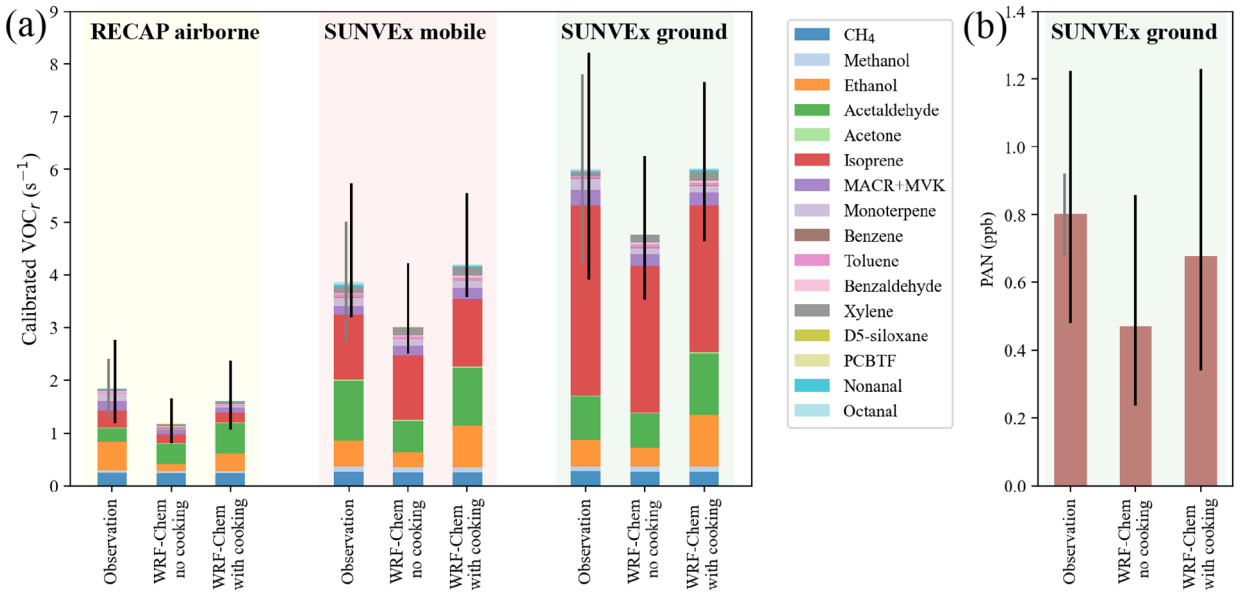

Figure 1. Cooking VOC emissions improves the model representation of VOC reactivity (VOC_r) and the NO_x temporary reservoir PAN. (a) Comparison of median speciated VOC_r between observations, including RECAP-CA airborne measurements (yellow), SUNVEx mobile measurements (red), SUNVEx ground measurements (green), and WRF-Chem simulations without and with cooking emissions. (b) Comparison of PAN between ground observations at Pasadena and WRF-Chem simulation without and with cooking VOC emissions. The black line represents the interquartile range of the summed calibrated VOC_r and PAN in either observations or model simulations. The gray line denotes the observational uncertainty: 30% for VOC_r and 15% for PAN.

2.3. Model. We utilize the Weather Research and Forecasting with Chemistry v4.2.2 (WRF-Chem) chemical transport model to simulate O_3 chemistry and evaluate the impact of the ZEV regulation on O_3. The model is configured with a horizontal spatial resolution of 4 × 4 km over California during the summer of 2021 (Figure S2). Detailed information regarding the model setup can be found in Zhu et al.,[29] with additional updates to the ozone boundary conditions described in Section S1.1.

The RACM2B-VCP chemical mechanism is developed for WRF-Chem and is capable of thoroughly evaluating the VOC chemistry in urban areas such as Los Angeles.[29] Here we update the RACM2B-VCP mechanism to the RACM2B-VCP2 mechanism by implementing the VOC chemistry emitted from cooking sources. The VOC speciation from cooking emissions is described in Coggon et al.,[28] including octanal, nonanal, acetic acid, acrolein, and higher-carbon aldehydes and acids. We add two lumped species, saturated cooking aldehydes and unsaturated cooking aldehydes, to distinguish them from aldehydes emitted from other emissions. In addition, we introduce two tracers as separate species into the RACM2B-VCP2 mechanism, nonanal and octanal, which are exclusively emitted from cooking emissions in the inventory. The reactions associated with these new species are summarized in Table S1 in Stockwell et al.[38] $P(O_3)$ is calculated online in each chemical time step, as described in Section S1.2.

2.4. Sensitivity Analysis. We conduct a series of model scenarios to explore the influence of cooking VOC emissions and ZEV adoption on O_3 pollution. First, we perform two model simulations differing only in the inclusion of cooking VOC emissions, covering the months of June, August, and the beginning of September 2021. Second, we simulate O_3 under model scenarios sequentially eliminating source sectors regulated by the ZEV adoption, including on-road gasoline, on-road diesel, off-road gasoline, and off-road diesel vehicle emissions. The particulate emissions from tire and brake wear from on-road vehicles are not reduced by ZEV adoption and are therefore unchanged in the sensitivity analysis. These simulations were conducted specifically for August 2021 to assess the impact of the ZEV policy on the level of O_3.

3. COOKING VOC EMISSIONS IMPROVE MODEL REPRESENTATION OF O_3 CHEMISTRY UNDER THE PRESENT-DAY EMISSION SCENARIO

We show that cooking accounts for as much as 28% of the mass of anthropogenic VOC emissions, which is greater than that from fossil fuels (20%), and constitutes half of the emissions from VCPs (52%) (Figure S3). The inclusion of cooking VOC emissions notably enhances the model representation of the VOC reactivity (VOC_r). VOC_r is defined as the sum of individual VOC concentrations multiplied by their reaction rates with hydroxyl radicals (OH), reflecting the collective contribution of diverse VOC species to the O_3 formation. Figure 1a compares calibrated VOC_r from two model simulations, with and without cooking VOC emissions, against RECAP-CA airborne measurements, SUNVEx mobile, and SUNVEx ground measurements. The calibrated VOC_r comprises 58% of the total VOC reactivity in WRF-Chem (Figure S4). We also evaluate model-simulated alkanes and formaldehyde in Section S2.3, accounting for 18% of the total VOC reactivity. Without cooking emissions, the model underpredicts calibrated VOC_r, as indicated by normalized median bias (NMDB) values ranging between −37 and −20% across these observation data sets, which is consistent with previous modeling studies in urban areas including LA.[29,35,39,40] Incorporating cooking emissions yields improved agreement between simulated and observed VOC_r considering a measurement uncertainty of 30%. NMDBs of VOC_r with cooking are −22, 8.2, and 3.2% compared against airborne, mobile, and ground measurements, respectively. The addition of cooking VOC emissions has the most significant impact on

https://doi.org/10.1021/acs.est.5c00902
Environ. Sci. Technol. 2025, 59, 5672−5682

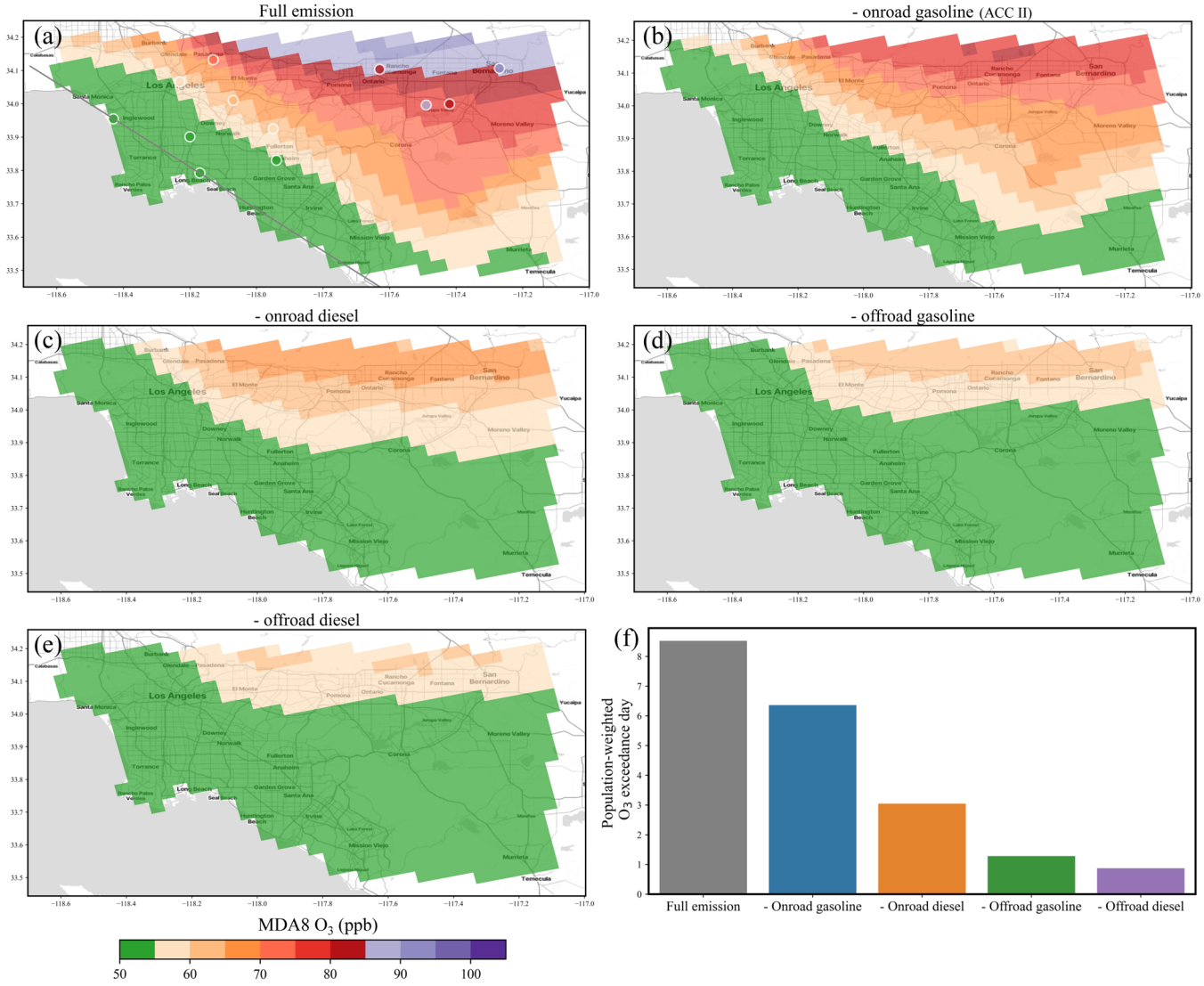

Figure 2. ZEV adoption substantially reduces MDA8 O_3 over LA and protects people from exposure to O_3 pollution. (a) Spatial distribution of MDA8 O_3 averaged in August 2021 from WRF-Chem simulation configured with full emission inventory. Circles denote the monthly MDA8 O_3 observed at 12 AQS monitoring sites. The gray line represents the coastline of LA defined in this study. (b–d) Spatial distributions of monthly average MDA8 O_3 simulated with source sectors sequentially eliminated, including on-road gasoline as per the ACC II regulation (b), on-road diesel (c), off-road gasoline (d), and off-road diesel emissions (e). (f) Changes in the average number of population-weighted O_3 exceedance days in August in LA under the present-day and ZEV sensitivity scenarios.

ethanol and acetaldehyde (Figure S6). Without cooking emissions, the model consistently underestimates ethanol across various observations, with NMDBs ranging between −75 and −30%. Conversely, incorporating cooking emissions aligns simulated ethanol concentrations more closely with observations, resulting in NMDBs within the range of −36 to 92%. Similarly, the inclusion of cooking emissions leads to a 30% increase in acetaldehyde, reducing NMDBs from −45 to −3.3% compared to SUNVEx mobile measurements and from −21 to 45% compared to SUNVEx ground measurements.

We also evaluate the model's skill in representing NO_x and its oxidation products. Previous work has demonstrated that our model simulation shows good agreement on NO_x concentration when compared against airborne measurements and satellite observations.[27,29] The oxidation of NO_x occurs concurrently with ozone production and results in various compound classes that act as either permanent sinks or temporary reservoirs of NO_x. We evaluate the model performance in representing NO_y in Section S2.2 and Figure S7. In addition, Figure 1b compares peroxy acetyl nitrate (PAN) between observations and two model simulations with and without cooking VOC emissions. PAN is a temporary NO_x reservoir and is used to evaluate the degree of urban pollution and its photochemical age. The absence of cooking emissions leads to substantial underpredictions of PAN, with an NMDB of −37%. Introducing cooking VOC emissions increases simulated PAN by 0.2 ppb primarily due to an increase in acetaldehyde, resulting in better agreement with ground observations, with an NMDB of −14%, which is within measurement uncertainty.

The influence of cooking VOC emissions on O_3 is relatively modest (Figures S12 and S13), however, they are essential for accurately representing the O_3 formation chemical regime over the LA Basin.[38] Using the box model described in Stockwell et al.[38] and recreated in Figure S11, ozone production in Pasadena is shown to be closer to transitioning to NO_x-

https://doi.org/10.1021/acs.est.5c00902
Environ. Sci. Technol. 2025, 59, 5672−5682

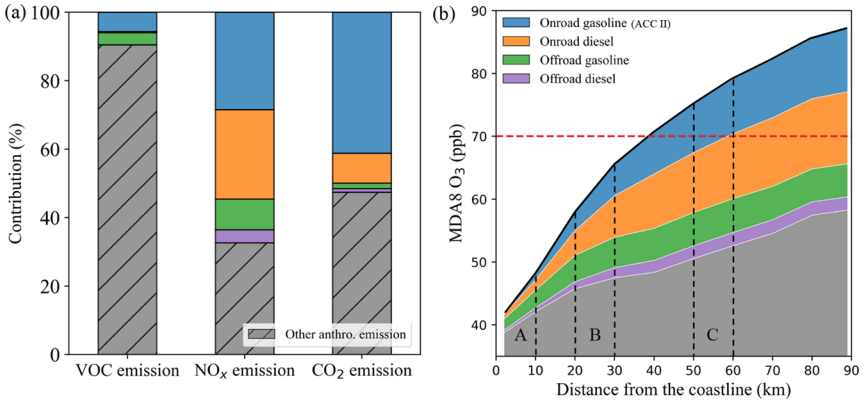

Figure 3. ZEV adoption reduces anthropogenic CO_2 emissions and O_3 pollution in the LA Basin. (a) Contribution of vehicle emissions associated with the ZEV adoption to total anthropogenic VOC, NO_x, and CO_2 emissions. (b) Monthly average MDA8 O_3 as a function of the distance to the coastline of LA. The solid black line represents the level of MDA8 O_3 under the baseline scenario. The dashed red line denotes the National Air Quality Standard for MDA8 O_3 of 70 ppb. The colored patches show the reduction on MDA8 O_3 if vehicle emissions are zeroed out progressively, including on-road gasoline as per the ACC II regulation (blue), on-road diesel (orange), off-road gasoline (green), and off-road diesel (purple) emissions. The black dashed lines denote three regions identified with distinct patterns of the O_3 chemical regimes described in Figure 4, encompassing 0−10, 20−30, and 50−60 km.

limited chemistry with the cooking VOC emissions, leading to 10% NO_x shifts in the transition point between NO_x-suppressed and NO_x-limited regimes.

With the updated present-day emission inventory including cooking VOC emissions, WRF-Chem captures the spatial variation in O_3 within the LA Basin (Figure 2a). We calculate the maximum daily 8-h average ozone (MDA8 O_3), a metric used to relate our results to the regulatory metric of 70 ppb MDA8 O_3 set by the US EPA to protect public health.[41] Shown in Figures 2a and S12b, we compare the August average MDA8 O_3 between the ground observations at 12 AQS sites and the WRF-Chem simulations. For each site, August MDA8 O_3 from the WRF-Chem simulation yields a good agreement with the observations, with the relative difference ranging between −4.0% and 23%. Notably, both observations and WRF-Chem simulations produce the positive gradient in the MDA8 O_3 between the coastline and inland LA Basin, as the difference in the August MDA8 O_3 between the two AQS sites, the West Los Angeles site (34.05°, −118.46°, 0.05km from the coastline) and the San Bernardino site (34.11°, −117.27°, 78km from the coastline), is as large as 44 ppb from the observations and 46 ppb from the WRF-Chem simulations. We calculate the number of O_3 exceedance days (i.e., MDA8 > 70 ppb) for each grid and then average them weighted by population, which is the same as that used in deriving emissions. On average, the LA population experiences 9 O_3 exceedance days in August (Figure 2f). Beyond the population-weighted average O_3 exceedance days, we further expand our analysis to quantify the population across different groups categorized by the number of O_3 exceedance days, highlighting the spatial variations in both O_3 pollution and its associated health impacts (Figure S15). Over 4 million people experience over 15 O_3 exceedance days in August, and over 1.6 million people are exposed to an O_3 exceedance for more than 25 days in August.

4. PHASING OUT GASOLINE EMISSIONS SUBSTANTIALLY REDUCES CO_2 EMISSIONS AND MODERATELY REDUCES O_3 POLLUTION

The ACC II regulation targets reducing emissions from on-road gasoline vehicles, such as passenger cars, including both combustion and evaporative gasoline emissions. The reduction in anthropogenic emissions of VOC, NO_x, and CO_2 resulting from ACC II regulation is illustrated in Figure 3a. In the LA basin, the ACC II regulation would lead to a local reduction of 41% of urban anthropogenic CO_2 emissions in August and highlights its capability to mitigate greenhouse gas emissions. ACC II regulation would also lead to a reduction in the emissions of primary pollutants, with a 29% reduction of anthropogenic NO_x emissions and a 5.6% reduction of anthropogenic VOC emissions.

The impact of the ACC II regulation on O_3 is quantified by using a model sensitivity analysis. In addition to the model simulation with the present-day emission inventory (referred to as "baseline scenario"), we conduct a second model simulation in the absence of on-road gasoline vehicle emissions, mirroring the emission scenario under the ACC II regulation (referred to as "ACC II scenario"). The change in monthly MDA8 O_3 due to the ACC II scenario is depicted in Figures 2b and S14. Compared with the baseline scenario (Figure 2a), the largest reduction of MDA8 O_3 is observed in the North Basin. As shown in Figure 3b, the reduction of MDA8 O_3 due to the ACC II regulation is aggregated as a function of the distance away from the coastline of LA. On-road gasoline emissions contribute to a moderate reduction in MDA8 O_3, and the average O_3 exceedance day weighted by population is 6 days, a 25% reduction compared to the present. Under the ACC II regulation, the influence on MDA8 O_3 near the coastline of LA is marginal while the largest reduction occurs in the most polluted region, 50−90 km away from the coastline, ranging from 7 to 10 ppb.

5. FURTHER ZEV ADOPTION ACCELERATES THE O_3 REDUCTION IN THE LA BASIN

While our results suggest that ACC II regulation moderately improves the ambient O_3 air quality, severe O_3 pollution is expected to persist in the LA Basin. The August MDA8 O_3 averages at 60 ppb over the LA Basin, ranging from 42 to 77 ppb (Figure 3b). 2.7 million people experience ozone exceedance over half of the month in August (Figure S15). We also test how further adoption of ZEVs for other sectors impacts O_3. We sequentially eliminate on-road diesel, off-road

https://doi.org/10.1021/acs.est.5c00902
Environ. Sci. Technol. 2025, 59, 5672−5682

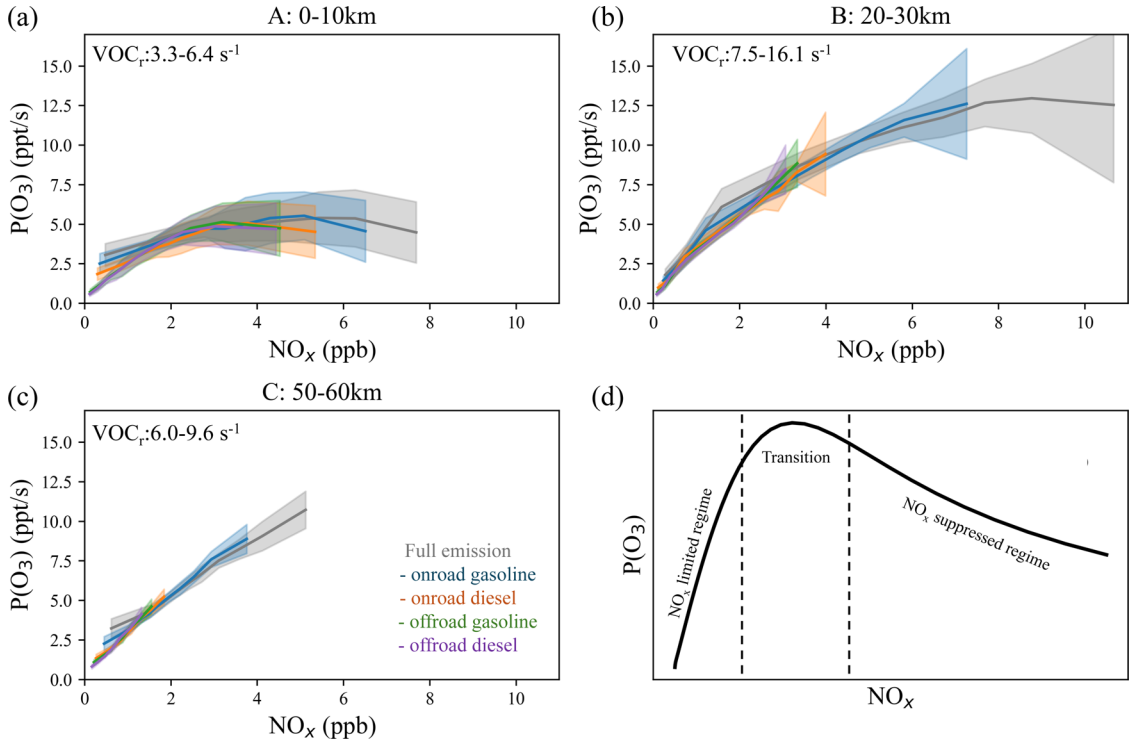

Figure 4. O_3 chemical regime shifts across LA due to the ZEV adoption. Panels (a–c) show the line plots depicting the relationship between instantaneous $P(O_3)$ and NO_x in model simulations with varying emission scenarios described in Figure 2a–e at the distance of 0–10 km (a), 20–30 km (b), and 50–60 km (c) from the coastline of LA. For each region, the relationship between $P(O_3)$ and NO_x within the interquartile range of VOC_r (specified in the upper left corner of each plot), is displayed at 1 pm local time for August. The line represents the mean $P(O_3)$ and the shaded line represents the standard deviation. Panel (d) presents a schematic of $P(O_3)$ as a function of NO_x at the photochemical steady state, illustrating the NO_x-limited regime, the NO_x-suppressed regime, and the transitional area in between. For panel (d), we assume a NO_2/NO ratio of 4, alkyl nitrate branching ratio (α) of 0.04, HO_x production rate of 0.3 ppt s^{-1}, and VOC_r of 5 s^{-1}.

gasoline, and off-road diesel following the ACC II regulation in a series of model sensitivity tests. The on-road diesel emissions include heavy-duty diesel trucks. Off-road emissions refer to fuel-based mobile engine sources that are not on roads, such as gasoline engines used in recreational vehicles, boats, and lawn equipment, as well as diesel engines used in agricultural and construction equipment.[34]

Figure 3a also shows the reduction of emissions attributed to further sequential ZEV adoption. The decrease in anthropogenic CO_2 emissions attributed to on-road diesel and off-road vehicle emissions is around a quarter of that of on-road gasoline emissions as per ACC II regulation, totaling 11% of the anthropogenic CO_2 emissions. Notably, the reduction in on-road diesel emissions leads to a 26% decrease in anthropogenic NO_x emissions, comparable to on-road gasoline emissions. A similar reduction in anthropogenic VOC emissions is expected from off-road (4%) and on-road (5.6%) gasoline emissions.

Figure 2c illustrates the simulated monthly MDA8 O_3 under on-road diesel scenarios. The regional average of MDA8 O_3 is decreased to 53 ppb. Shown in Figure 3b, the sequential decrease in on-road diesel emission ranges from 0.7 to 11 ppb from the coastline of LA to the East Basin. Following the implementation of ACC II regulation and further control on on-road diesel emission, the largest August average MDA8 O_3 over the LA Basin is 64 ppb, leading to the O_3 level over the whole LA Basin below the NAAQS. The average population-weighted days of O_3 exceedance are substantially reduced to 3 days in August (Figure 2f). No population in LA is exposed to ozone exceedance for over 15 days, while 1.3 million people still experience 5–15 O_3 exceedance days in August (Figure S15).

Figure 2d,e illustrates the simulated monthly MDA8 O_3 under off-road gasoline and off-road diesel scenarios. The impact of reducing off-road gasoline vehicle emissions on MDA8 O_3 ranges from 2 ppb near the coastline to 5 ppb in the Northeast Basin. Reducing off-road diesel vehicle emissions decreases the regional average MDA8 O_3 by 1.6 ppb, with the largest reduction observed in the East Basin by 2.2 ppb. With the ZEV adoption for all mobile source engines, the number of days of O_3 exceedance in August is 1 day on average for the people of LA (Figure 2f).

6. ZEV ADOPTION LEADS TO SHIFTS IN THE O_3 FORMATION CHEMICAL REGIME

To determine the local O_3 formation chemical regime, we collect simulated daily instantaneous O_3 production rate ($P(O_3)$), NO_x, and VOC_r at 1 pm local time in three regions located 0–10, 20–30, and 50–60 km from the LA coastline. Because the mixture of NO_x and VOC_r determines the chemical regime of O_3 production, in each selected regime, we show the relationship between $P(O_3)$ and NO_x, within the interquartile range of VOC_r in Figure 4a–c. The distributions of $P(O_3)$ and NO_x under the conditions below the 25th and above the 75th quantile ranges of VOC_r are shown in Figures S19 and S20.

As the anthropogenic VOC emissions stay relatively constant compared to the anthropogenic NO_x emissions, the moderate reduction in O_3 pollution with the ACC II regulation

https://doi.org/10.1021/acs.est.5c00902
Environ. Sci. Technol. 2025, 59, 5672–5682

underscores the nonlinearity between $P(O_3)$ and NO_x. As shown in Figure 4d, with constant VOC_r, the urban environment falls into the NO_x-limited regime under low NO_x conditions, with a consistent increase in $P(O_3)$ alongside an increase in NO_x. Conversely, under high NO_x conditions, the relationship between $P(O_3)$ and NO_x is the opposite, indicating a NO_x-suppressed regime.

In regions within 10 km and 20−30 km of the coastline of LA, $P(O_3)$ and NO_x exhibit distinct nonlinearity under the baseline scenario, indicating the transition between NO_x-suppressed regime and NO_x-limited regime. Therefore, relatively small changes in O_3 pollution are shown with a substantial reduction in NO_x emissions under the ACC II regulation. In contrast, the East Basin, 50−60 km from the coastline, falls into the NO_x-limited regime under the baseline scenario, resulting in a larger O_3 reduction in the East Basin than in the West Basin under the ACC II regulation.

With the implementation of the ACC II regulation, most of the LA Basin switches to a NO_x-limited regime, which is significant because any further NO_x reduction strategy like reducing on-road diesel, off-road gasoline, off-road diesel, or other sector (e.g., industry) emissions will efficiently lower ozone. Additionally, shifting most of the LA basin to NO_x-limited is important for controlling O_3 in the East Basin where the level of pollution with O_3 is the highest because O_3 is not only locally produced here but also transported from the west. The only exception is that the coastal region remains in the transition regime because of relatively high NO_x levels under conditions of low VOC_r, due to major shipping ports, a dense highway network,[27] and low boundary layer height (Figure S17).

7. DISCUSSION

The sensitivity of O_3 to reductions in NO_x and VOCs has been a central focus for determining the most effective strategy for controlling the level of O_3 pollution. Recent studies have delved into noncombustion anthropogenic VOC emissions in urban areas, including VCPs[42−44] and cooking activities.[28] Our analysis reveals that VCP and cooking sources are major contributors to anthropogenic VOC sources, accounting for 80% of total anthropogenic VOC emissions by mass in LA. The inclusion of missing emissions into chemical models is needed to accurately represent VOC_r and the VOC/NO_x mixture that determines ozone sensitivity. Without these anthropogenic VOC emissions, models suggest that the Los Angeles Basin is NO_x-suppressed. However, when these VOCs are fully implemented in emissions inventories and chemical mechanisms, ozone production is shown to be closer to transitioning to NO_x-limited chemistry in Pasadena during peak production (e.g., Stockwell et al.,[38] Peischl et al.,[45] Figure S11). This regime is where NO_x reductions are most effective in reducing ozone pollution.

However, the impact of these anthropogenic VOC emissions on O_3 levels is relatively small. Prior research has shown that VCP emissions contribute to a 3−6 ppb increment in MDA8 O_3.[29,38,44] Biogenic VOC emissions, contributing more than half of the total VOC reactivity (VOC_r),[29,35,46] are dominated by meteorological conditions. While future urban greening programs could prioritize tree species featuring low VOC emissions,[47] reducing VOC emissions to achieve lower O_3 levels presents a greater challenge compared to reducing NO_x emissions, which are predominantly from anthropogenic vehicle emissions in urban areas.

In this study, we demonstrate that ZEV adoption, not only on gasoline cars but also on diesel trucks and off-road engines, can effectively reduce the level of O_3 pollution in parallel to mitigating CO_2 emissions. With the implementation of the ACC II regulation, a significant portion of LA transitions to the NO_x-limited regime, highlighting its effectiveness in controlling O_3 levels by reducing NO_x emissions. Moreover, NO_x emission control through ZEV adoption may be a simpler mitigation strategy than reducing VOC emissions due to a large fraction of VOC emissions being biogenic and from nonvehicular anthropogenic sources. As a city with a long history of severe O_3 pollution in the United States, LA serves as a testbed for evaluating the effectiveness of the O_3 control policies while also mitigating GHG emissions.

■ ASSOCIATED CONTENT

Supporting Information

The observational data from SUNVEx and RECAP-CA field campaigns are available at https://csl.noaa.gov/projects/sunvex/. Emissions for each scenario and gridded cooking emissions are publicly accessible at https://csl.noaa.gov/groups/csl7/measurements/2021sunvex/emissions/. The analysis data set is available at https://csl.noaa.gov/groups/csl4/modeldata/data/Zhu2024/. The WRF-Chem source codes and the analysis codes are available at https://github.com/NOAA-CSL/WRF-Chem_CSL_Publications/tree/main/Qindan_Zhu_et_al_2024. The Supporting Information is available free of charge at https://pubs.acs.org/doi/10.1021/acs.est.5c00902.

WRF-Chem model configuration: O_3 boundary condition; calculation of instaneous ozone production rate in WRF-Chem; steady state OH model; validation of cooking emission; evaluation of model simulated NO_y; evaluation of model simulated alkanes and formaldehyde; impact of cooking VOC emissions on O_3; impact of scaling ethanol in cooking VOC emissions; changes in NO_x and VOC_r due to the ZEV adoption; list of instruments and the corresponding measured species used in our study from RECAP and SUNVEx field campaigns; O_3 vertical profile observed during Atom-1 airborne observations, compared against original and adjusted chemical O_3 boundary condition ("BC") used in the WRF-Chem configuration; reactions included in WRF-Chem for $P(O_3)$ calculation; model domain defined in our WRF-Chem simulation at the spatial resolution of 4 km; mass distribution of anthropogenic VOC emissions averaged in the LA Basin; budget of total surface VOC reactivity averaged over the LA Basin in August; comparison of nonanal (a) and octanal (b) between observations and WRF-Chem simulation with cooking VOC emissions; comparison of ethanol (a) and aldehyde (b) between observations and WRF-Chem simulations without cooking emissions, with cooking emissions, and with cooking emissions excluding scaling up ethanol; comparison of the diurnal cycle of NO_y components and PBL heights between 9 and 19 local time; mapping between WRF-Chem simulated alkane and measurements by GCMS at ground site Pasadena during the SUNVEX field campaign; comparison of ethanes (a), alkanes with carbon numbers 3−4 (b), alkanes with carbon numbers 5−7 (c), and alkanes with carbon numbers larger than 7 (d) between ground

https://doi.org/10.1021/acs.est.5c00902
Environ. Sci. Technol. 2025, 59, 5672−5682

observations at Pasadena and WRF-Chem simulation with cooking VOC emissions; comparison of HCHO in WRF-Chem simulations against the observations at 5 South Coast AQMD monitoring sites in August 2021; comparison of HCHO between SCAQMD monitoring sites and WRF-Chem simulation with cooking emissions; comparison of VOC_r and PAN between observations and WRF-Chem simulations without cooking emissions, with cooking emissions, and with cooking emissions without scaling up ethanol; change in MDA8 O3 in Pasadena as NOx is scaled from its initial mixing ratio in box model, considering the inclusion or exclusion of cooking emissions and the scaling of ethanol emissions; comparison of observed MDA8 O_3 to WRF-Chem with and without cooking emissions; contribution of cooking VOC emissions to the monthly average MDA8 O_3 as a function of the distance to the coastline of LA; distribution of vehicle emissions associated with the ZEV adoption to MDA8 O_3 as a function of the distance to the coastline of LA; LA population exposed to varying numbers of ozone exceedance days in August; NO_x (a) and VOC_r (b) as a function of the distance to the coastline of LA under baseline, on-road gasoline, on-road diesel, off-road gasoline, and off-road diesel emissions scenarios; boundary layer height as a function of the distance to the coastline of LA under baseline scenarios; density distribution of VOC_r at distances of 0−10 km, 20−30 km, and 50−60 km from the coastline of LA; relationship between $P(O_3)$ and NO_x in model simulations with varying emission scenarios with the VOC_r above the 25th quantile; and relationship between $P(O_3)$ and NO_x in model simulations with varying emission scenarios with the VOC_r above the 75th quantile (PDF)

AUTHOR INFORMATION

Corresponding Authors

Qindan Zhu − *NOAA Chemical Sciences Laboratory, Boulder, Colorado 80305, United States; Cooperative Institute for Research in Environmental Sciences, University of Colorado, Boulder, Colorado 80309, United States;* Present Address: Department of Earth, Atmospheric and Planetary Sciences, Massachusetts Institute of Technology, Cambridge, Massachusetts 02139, United States; orcid.org/0000-0003-2173-4014; Email: qdzhu@mit.edu

Rebecca H. Schwantes − *NOAA Chemical Sciences Laboratory, Boulder, Colorado 80305, United States;* orcid.org/0000-0002-7095-3718; Email: rebecca.schwantes@noaa.gov

Authors

Chelsea E. Stockwell − *NOAA Chemical Sciences Laboratory, Boulder, Colorado 80305, United States;* orcid.org/0000-0003-3462-2126

Colin Harkins − *NOAA Chemical Sciences Laboratory, Boulder, Colorado 80305, United States; Cooperative Institute for Research in Environmental Sciences, University of Colorado, Boulder, Colorado 80309, United States;* orcid.org/0000-0001-5692-3427

Congmeng Lyu − *NOAA Chemical Sciences Laboratory, Boulder, Colorado 80305, United States; Cooperative Institute for Research in Environmental Sciences, University of Colorado, Boulder, Colorado 80309, United States;* orcid.org/0000-0002-6946-7835

Matthew Coggon − *NOAA Chemical Sciences Laboratory, Boulder, Colorado 80305, United States;* orcid.org/0000-0002-5763-1925

Katelyn A. Yu − *Department of Civil and Environmental Engineering, University of California, Berkeley, Berkeley, California 94720, United States;* orcid.org/0000-0002-1462-3511

Carsten Warneke − *NOAA Chemical Sciences Laboratory, Boulder, Colorado 80305, United States;* orcid.org/0000-0003-3811-8496

Jordan Schnell − *Cooperative Institute for Research in Environmental Sciences, University of Colorado, Boulder, Colorado 80309, United States; NOAA Global Systems Laboratory, Boulder, Colorado 80305, United States*

Jian He − *NOAA Chemical Sciences Laboratory, Boulder, Colorado 80305, United States; Cooperative Institute for Research in Environmental Sciences, University of Colorado, Boulder, Colorado 80309, United States*

Havala O. T. Pye − *Office of Research and Development, U.S. Environmental Protection Agency, Research Triangle Park, North Carolina 27711, United States;* orcid.org/0000-0002-2014-2140

Meng Li − *NOAA Chemical Sciences Laboratory, Boulder, Colorado 80305, United States; Cooperative Institute for Research in Environmental Sciences, University of Colorado, Boulder, Colorado 80309, United States*

Ravan Ahmadov − *NOAA Global Systems Laboratory, Boulder, Colorado 80305, United States;* orcid.org/0000-0002-6996-7071

Eva Y. Pfannerstill − *Department of Environmental Science, Policy, and Management, University of California, Berkeley, Berkeley, California 94720, United States;* Present Address: Institute for Climate and Energy Systems 3: Troposphere, Forschungszentrum Jülich, 52425 Jülich, Germany.; orcid.org/0000-0001-7715-1200

Bryan Place − *Office of Research and Development, U.S. Environmental Protection Agency, Research Triangle Park, North Carolina 27711, United States*

Paul Wooldridge − *Department of Chemistry, University of California, Berkeley, Berkeley, California 94720, United States*

Benjamin C. Schulze − *Department of Environmental Science and Engineering, California Institute of Technology, Pasadena, California 91125, United States;* orcid.org/0000-0002-6405-8872

Caleb Arata − *Department of Civil and Environmental Engineering, University of California, Berkeley, Berkeley, California 94720, United States*

Anthony Bucholtz − *Department of Meteorology, Naval Postgraduate School, Monterey, California 93943, United States*

John H. Seinfeld − *Department of Environmental Science and Engineering, California Institute of Technology, Pasadena, California 91125, United States;* orcid.org/0000-0003-1344-4068

Lu Xu − *NOAA Chemical Sciences Laboratory, Boulder, Colorado 80305, United States; Cooperative Institute for Research in Environmental Sciences, University of Colorado, Boulder, Colorado 80309, United States;* Present Address: Department of Energy, Environmental and Chemical Engineering, Washington University in St.

https://doi.org/10.1021/acs.est.5c00902
Environ. Sci. Technol. 2025, 59, 5672−5682

Louis, Missouri 63130, United States.; orcid.org/0000-0002-0021-9876
Kristen Zuraski − *NOAA Chemical Sciences Laboratory, Boulder, Colorado 80305, United States; Cooperative Institute for Research in Environmental Sciences, University of Colorado, Boulder, Colorado 80309, United States;* orcid.org/0000-0003-3149-6611
Michael A. Robinson − *NOAA Chemical Sciences Laboratory, Boulder, Colorado 80305, United States; Cooperative Institute for Research in Environmental Sciences, University of Colorado, Boulder, Colorado 80309, United States*
J. Andrew Neuman − *NOAA Chemical Sciences Laboratory, Boulder, Colorado 80305, United States*
Jessica Gilman − *NOAA Chemical Sciences Laboratory, Boulder, Colorado 80305, United States;* orcid.org/0000-0002-7899-9948
Aaron Lamplugh − *NOAA Chemical Sciences Laboratory, Boulder, Colorado 80305, United States; Cooperative Institute for Research in Environmental Sciences, University of Colorado, Boulder, Colorado 80309, United States;* Present Address: Air Pollution Control Division, Colorado Department of Public Health and Environment, Denver, Colorado 80246, United States.; orcid.org/0000-0002-5131-7070
Patrick R. Veres − *NOAA Chemical Sciences Laboratory, Boulder, Colorado 80305, United States;* Present Address: Research Aviation Facility, National Center for Atmospheric Research, Boulder, Colorado 80301, United States.
Jeff Peischl − *NOAA Chemical Sciences Laboratory, Boulder, Colorado 80305, United States; Cooperative Institute for Research in Environmental Sciences, University of Colorado, Boulder, Colorado 80309, United States;* orcid.org/0000-0002-9320-7101
Andrew Rollins − *NOAA Chemical Sciences Laboratory, Boulder, Colorado 80305, United States*
Steven S. Brown − *NOAA Chemical Sciences Laboratory, Boulder, Colorado 80305, United States; Department of Chemistry, University of Colorado, Boulder, Colorado 80309, United States;* orcid.org/0000-0001-7477-9078
Allen H. Goldstein − *Department of Environmental Science, Policy, and Management and Department of Civil and Environmental Engineering, University of California, Berkeley, Berkeley, California 94720, United States;* orcid.org/0000-0003-4014-4896
Ronald C. Cohen − *Department of Chemistry and Department of Earth and Planetary Sciences, University of California, Berkeley, Berkeley, California 94720, United States;* orcid.org/0000-0001-6617-7691
Brian C. McDonald − *NOAA Chemical Sciences Laboratory, Boulder, Colorado 80305, United States;* orcid.org/0000-0001-8600-5096

Complete contact information is available at: https://pubs.acs.org/10.1021/acs.est.5c00902

Notes

The authors declare no competing financial interest.

■ ACKNOWLEDGMENTS

Q.Z. was supported by the NOAA Climate & Global Change Postdoc Fellowship. MMC, CES, QZ, and RHS received support from the U.S. Environmental Protection Agency (EPA) STAR program (grant # 84001001). The views expressed in this document are solely those of the authors and do not necessarily reflect those of the U.S. Environmental Protection Agency. EPA does not endorse any products or commercial services mentioned in this publication. The statements, findings, conclusions, and recommendations are those of the author(s) and do not necessarily reflect the views of NOAA or the U.S. Department of Commerce. The RECAP-CA field campaign was funded by California Air Resources Board Contract number 20RD003, 20AQP012, and the Presidential Early Career Award for Scientists and Engineers (PECASE)(from Brian McDonald). The SUNVEx field campaign was funded in part by the California Air Resources Board (grant no. 20RD002); and the Cooperative Institute for Research in Environmental Sciences (grant nos. NA17OAR4320101 and NA22OAR4320151). We also thank NOAA's High-Performance Computing Program. This research was supported in part by the NOAA cooperative agreement NA22OAR4320151, for the Cooperative Institute for Earth System Research and Data Science (CIESRDS).

■ REFERENCES

(1) Jacob, D. J. Heterogeneous chemistry and tropospheric ozone. *Atmos. Environ.* **2000**, *34*, 2131−2159.
(2) Krewski, D.; Jerrett, M.; Burnett, R. T.; Ma, R.; Hughes, E.; Shi, Y.; Turner, M. C.; Pope, III, C. A.; Thurston, G.; Calle, E. E. *Extended follow-up and spatial analysis of the American Cancer Society study linking particulate air pollution and mortality*; Health Effects Institute: Boston, MA, 2009; Vol. *140*.
(3) Lim, S. S.; Vos, T.; Flaxman, A. D.; Danaei, G.; Shibuya, K.; Adair-Rohani, H.; AlMazroa, M. A.; Amann, M.; Anderson, H. R.; Andrews, K. G.; et al. A comparative risk assessment of burden of disease and injury attributable to 67 risk factors and risk factor clusters in 21 regions, 1990−2010: a systematic analysis for the Global Burden of Disease Study 2010. *lancet* **2012**, *380*, 2224−2260.
(4) Hoek, G.; Krishnan, R. M.; Beelen, R.; Peters, A.; Ostro, B.; Brunekreef, B.; Kaufman, J. D. Long-term air pollution exposure and cardio-respiratory mortality: a review. *Environ. Health* **2013**, *12*, 43.
(5) Burnett, R. T.; Pope, C. A., III; Ezzati, M.; Olives, C.; Lim, S. S.; Mehta, S.; Shin, H. H.; Singh, G.; Hubbell, B.; Brauer, M.; et al. An integrated risk function for estimating the global burden of disease attributable to ambient fine particulate matter exposure. *Environ. Health Perspect.* **2014**, *122*, 397−403.
(6) Burnett, R.; Chen, H.; Szyszkowicz, M.; Fann, N.; Hubbell, B.; Pope, C. A., III; Apte, J. S.; Brauer, M.; Cohen, A.; Weichenthal, S.; et al. Global estimates of mortality associated with long-term exposure to outdoor fine particulate matter. *Proc. Natl. Acad. Sci. U. S. A.* **2018**, *115*, 9592−9597.
(7) Dedoussi, I. C.; Eastham, S. D.; Monier, E.; Barrett, S. R. Premature mortality related to United States cross-state air pollution. *Nature* **2020**, *578*, 261−265.
(8) EPA. *Total U.S. Greenhouse Gas Emissions by Economic Sector in 2022*, 2022; https://www.epa.gov/ghgemissions/sources-greenhouse-gas-emissions, last accessed April 24, 2024.
(9) IPCC. In *Climate Change 2023: Synthesis Report. Contribution of Working Groups I, II and III to the Sixth Assessment Report of the Intergovernmental Panel on Climate Change*; Core Writing Team, H. L., J, R., Eds.; Cambridge University Press: Geneva, Switzerland, 2023; pp 1−34.
(10) USGCRP, U. G. C. R. P. In *Impacts, risks, and adaptation in the United States: Fourth National Climate Assessment, volume II*, Reidmiller, C. A. D. E. K. K. K. L. T. M., D, R., B, S., Eds., 2018.
(11) Westerling, A. L. Increasing western US forest wildfire activity: sensitivity to changes in the timing of spring. *Philosophical Transactions of the Royal Society B: Biological Sciences* **2016**, *371*, 20150178.

(12) EPA. *O3 nonattainment area*, 2024; https://www3.epa.gov/airquality/greenbook/map8hr_2015.html, last accessed October 28, 2021.
(13) Williams, J. H.; DeBenedictis, A.; Ghanadan, R.; Mahone, A.; Moore, J.; Morrow, W. R., III; Price, S.; Torn, M. S. The technology path to deep greenhouse gas emissions cuts by 2050: the pivotal role of electricity. *science* **2012**, *335*, 53−59.
(14) Office of Governor Kathy Hochul, N. Governor Hochul Drives Forward New York's Transition to Clean Transportation, 2022; https://ogs.ny.gov/zero-emission-vehicles-infrastructure-0, last accessed March 23, 2024.
(15) MA Department of Energy Resources, M. Climate Leader Communities GUIDANCE: Zero-Emission-First Vehicle Policy, 2023; https://www.mass.gov/doc/climate-leader-communities-zev-first-policy/download, last accessed March 23, 2024.
(16) Department for Transport U.K, U. Transitioning to zero-emission cars and vans: 2035 delivery plan. 2022; https://www.gov.uk/government/publications/transitioning-to-zero-emission-cars-and-vans-2035-delivery-plan, last accessed March 23, 2024.
(17) Council of the European Union, E. First 'Fit for 55' proposal agreed: the EU strengthens targets for CO2 emissions for new cars and vans, 2022; https://www.consilium.europa.eu/en/press/press-releases/2022/10/27/first-fit-for-55-proposal-agreed-the-eu-strengthens-targets-for-co2-emissions-for-new-cars-and-vans/, last accessed March 23, 2024.
(18) Zhu, S.; Horne, J. R.; Mac Kinnon, M.; Samuelsen, G.; Dabdub, D. Comprehensively assessing the drivers of future air quality in California. *Environ. Int.* **2019**, *125*, 386−398.
(19) Peters, D. R.; Schnell, J. L.; Kinney, P. L.; Naik, V.; Horton, D. E. Public Health and Climate Benefits and Trade-Offs of U.S. Vehicle Electrification. *GeoHealth* **2020**, *4*, No. e2020GH000275.
(20) Skipper, T. N.; Lawal, A. S.; Hu, Y.; Russell, A. G. Air quality impacts of electric vehicle adoption in California. *Atmos. Environ.* **2023**, *294*, No. 119492.
(21) Chang, S. Y.; Huang, J.; Chaveste, M. R.; Lurmann, F. W.; Eisinger, D. S.; Mukherjee, A. D.; Erdakos, G. B.; Alexander, M.; Knipping, E. Electric vehicle fleet penetration helps address inequalities in air quality and improves environmental justice. *Commun. Earth Environ.* **2023**, *4*, 135.
(22) Yu, Q.; He, B. Y.; Ma, J.; Zhu, Y. California's zero-emission vehicle adoption brings air quality benefits yet equity gaps persist. *Nat. Commun.* **2023**, *14*, 7798.
(23) Zhu, S.; Mac Kinnon, M.; Carlos-Carlos, A.; Davis, S. J.; Samuelsen, S. Decarbonization will lead to more equitable air quality in California. *Nat. Commun.* **2022**, *13*, 5738.
(24) Mousavinezhad, S.; Choi, Y.; Khorshidian, N.; Ghahremanloo, M.; Momeni, M. Air quality and health co-benefits of vehicle electrification and emission controls in the most populated United States urban hubs: Insights from New York, Los Angeles, Chicago, and Houston. *Science of The Total Environment* **2024**, *912*, No. 169577.
(25) Li, Y.; Ravi, V.; Heath, G.; Zhang, J.; Vahmani, P.; Lee, S.-M.; Zhang, X.; Sanders, K. T.; Ban-Weiss, G. A. Air quality and public health co-benefits of 100% renewable electricity adoption and electrification pathways in Los Angeles. *Environmental Research Letters* **2024**, *19*, No. 034015.
(26) Schnell, J. L.; Naik, V.; Horowitz, L. W.; Paulot, F.; Ginoux, P.; Zhao, M.; Horton, D. E. Air quality impacts from the electrification of light-duty passenger vehicles in the United States. *Atmos. Environ.* **2019**, *208*, 95−102.
(27) Yu, K. A.; Li, M.; Harkins, C.; He, J.; Zhu, Q.; Verreyken, B.; Schwantes, R. H.; Cohen, R. C.; McDonald, B. C.; Harley, R. A. Improved Spatial Resolution in Modeling of Nitrogen Oxide Concentrations in the Los Angeles Basin. *Environ. Sci. Technol.* **2023**, *57*, 20689−20698.
(28) Coggon, M. M.; Stockwell, C. E.; Xu, L.; Peischl, J.; Gilman, J. B.; Lamplugh, A.; Bowman, H. J.; Aikin, K.; Harkins, C.; Zhu, Q.; et al. Contribution of cooking emissions to the urban volatile organic compounds in Las Vegas. *NV. Atmospheric Chemistry and Physics* **2024**, *24*, 4289−4304.
(29) Zhu, Q.; Schwantes, R. H.; Coggon, M.; Harkins, C.; Schnell, J.; He, J.; Pye, H. O.; Li, M.; Baker, B.; Moon, Z.; et al. A better representation of VOC chemistry in WRF-Chem and its impact on ozone over Los Angeles. *Atmos. Chem. Phys.* **2024**, *24*, 5265−5286.
(30) Pfannerstill, E. Y.; Arata, C.; Zhu, Q.; Schulze, B. C.; Woods, R.; Seinfeld, J. H.; Bucholtz, A.; Cohen, R. C.; Goldstein, A. H. Volatile organic compound fluxes in the agricultural San Joaquin Valley − spatial distribution, source attribution, and inventory comparison. *Atmospheric Chemistry and Physics* **2023**, *23*, 12753−12780.
(31) Nussbaumer, C. M.; Place, B. K.; Zhu, Q.; Pfannerstill, E. Y.; Wooldridge, P.; Schulze, B. C.; Arata, C.; Ward, R.; Bucholtz, A.; Seinfeld, J. H.; Goldstein, A. H.; Cohen, R. C. Measurement report: Airborne measurements of NO_x fluxes over Los Angeles during the RECAP-CA 2021 campaign. *Atmospheric Chemistry and Physics* **2023**, *23*, 13015−13028.
(32) Baker, B.; Pan, L. Overview of the model and observation evaluation toolkit (MONET) version 1.0 for evaluating atmospheric transport models. *Atmosphere* **2017**, *8*, 210.
(33) Lyu, C.; Harkins, C.; Li, M.; McDonald, B.; Prothero, J.; Mueller, K. The U. S. Greenhouse Gas and Air Pollutant Emissions System (GRA2PES); National Institute of Standards and Technology (NIST), 2024.
(34) Harkins, C.; McDonald, B. C.; Henze, D. K.; Wiedinmyer, C. A fuel-based method for updating mobile source emissions during the COVID-19 pandemic. *Environmental Research Letters* **2021**, *16*, No. 065018.
(35) Pfannerstill, E. Y.; Arata, C.; Zhu, Q.; Schulze, B. C.; Woods, R.; Harkins, C.; Schwantes, R. H.; McDonald, B. C.; Seinfeld, J. H.; Bucholtz, A.; et al. Comparison between Spatially Resolved Airborne Flux Measurements and Emission Inventories of Volatile Organic Compounds in Los Angeles. *Environ. Sci. Technol.* **2023**, *57*, 15533−15545.
(36) Arata, C.; Misztal, P. K.; Tian, Y.; Lunderberg, D. M.; Kristensen, K.; Novoselac, A.; Vance, M. E.; Farmer, D. K.; Nazaroff, W. W.; Goldstein, A. H. Volatile organic compound emissions during HOMEChem. *Indoor Air* **2021**, *31*, 2099−2117.
(37) Farmer, D. K.; Vance, M. E.; Abbatt, J. P.; Abeleira, A.; Alves, M. R.; Arata, C.; Boedicker, E.; Bourne, S.; Cardoso-Saldaña, F.; Corsi, R.; et al. Overview of HOMEChem: House observations of microbial and environmental chemistry. *Environmental Science: Processes & Impacts* **2019**, *21*, 1280−1300.
(38) Stockwell, C. E.; Coggon, M. M.; Schwantes, R. H.; Harkins, C.; Verreyken, B.; Lyu, C.; Zhu, Q.; Xu, L.; Gilman, J. B.; Lamplugh, A.; et al. Urban ozone formation and sensitivities to volatile chemical products, cooking emissions, and NO x across the Los Angeles Basin. *EGUsphere* **2024**, *2024*, 1−24.
(39) Griffith, S. M.; Hansen, R.; Dusanter, S.; Michoud, V.; Gilman, J.; Kuster, W.; Veres, P.; Graus, M.; De Gouw, J.; Roberts, J.; et al. Measurements of hydroxyl and hydroperoxy radicals during CalNex-LA: Model comparisons and radical budgets. *Journal of Geophysical Research: Atmospheres* **2016**, *121*, 4211−4232.
(40) Hansen, R.; Griffith, S.; Dusanter, S.; Gilman, J.; Graus, M.; Kuster, W.; Veres, P.; de Gouw, J.; Warneke, C.; Washenfelder, R.; et al. Measurements of Total OH Reactivity During CalNex-LA. *J. Geophys. Res.: Atmos.* **2021**, *126*, No. e2020JD032988.
(41) EPA, National Ambient Air Quality Standards for Ozone, 2015; https://www.govinfo.gov/content/pkg/FR-2015-10-26/pdf/2015-26594.pdf, last accessed July 12, 2024.
(42) McDonald, B. C.; De Gouw, J. A.; Gilman, J. B.; Jathar, S. H.; Akherati, A.; Cappa, C. D.; Jimenez, J. L.; Lee-Taylor, J.; Hayes, P. L.; McKeen, S. A.; et al. Volatile chemical products emerging as largest petrochemical source of urban organic emissions. *Science* **2018**, *359*, 760−764.
(43) Coggon, M. M.; Gkatzelis, G. I.; McDonald, B. C.; Gilman, J. B.; Schwantes, R. H.; Abuhassan, N.; Aikin, K. C.; Arend, M. F.; Berkoff, T. A.; Brown, S. S.; et al. Volatile chemical product emissions

https://doi.org/10.1021/acs.est.5c00902
Environ. Sci. Technol. 2025, 59, 5672−5682

enhance ozone and modulate urban chemistry. *Proc. Natl. Acad. Sci. U. S. A.* **2021**, *118*, No. e2026653118.
(44) Qin, M.; Murphy, B. N.; Isaacs, K. K.; McDonald, B. C.; Lu, Q.; McKeen, S. A.; Koval, L.; Robinson, A. L.; Efstathiou, C.; Allen, C.; et al. Criteria pollutant impacts of volatile chemical products informed by near-field modelling. *Nature sustainability* **2021**, *4*, 129−137.
(45) Peischl, J.; Aikin, K. C.; McDonald, B. C.; Harkins, C.; Middlebrook, A. M.; Langford, A. O.; Cooper, O. R.; Chang, K.-L.; Brown, S. S. Quantifying anomalies of air pollutants in 9 US cities during 2020 due to COVID-19 lockdowns and wildfires based on decadal trends. *Elementa* **2023**, *11*, No. 00029.
(46) Pfannerstill, E. Y.; Arata, C.; Zhu, Q.; Schulze, B. C.; Ward, R.; Woods, R.; Harkins, C.; Schwantes, R. H.; Seinfeld, J. H.; Bucholtz, A.; et al. Temperature-dependent emissions dominate aerosol and ozone formation in Los Angeles. *Science* **2024**, *384*, 1324−1329.
(47) Gu, S.; Guenther, A.; Faiola, C. Effects of anthropogenic and biogenic volatile organic compounds on Los Angeles air quality. *Environ. Sci. Technol.* **2021**, *55*, 12191−12201.

https://doi.org/10.1021/acs.est.5c00902
Environ. Sci. Technol. 2025, 59, 5672−5682